Analyst

Accepted Manuscript

This article can be cited before page numbers have been issued, to do this please use: B. Veigas, A. Matias, T. R. Calmeiro, E. Fortunato, A. Fernandes and P. V. Baptista, *Analyst*, 2019, DOI: 10.1039/C9AN00319C.

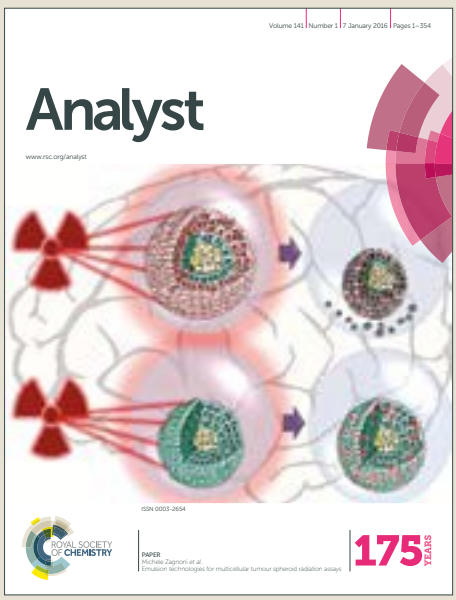

ROYAL SOCIETY OF CHEMISTRY

rsc.li/analyst

View Article Online
DOI: 10.1039/C9AN00319C

ARTICLE

Antibody Modified Gold Nanoparticles for Fast Colorimetric screening of Rheumatoid arthritis

Received 00th January 20xx,
Accepted 00th January 20xx

DOI: 10.1039/x0xx00000x

Bruno Veigas,[a,b] Ana Matias,[a] Tomás Calmeiro,[b] Elvira Fortunato,[b] Alexandra R. Fernandes[a] and Pedro Viana Baptista*[a]

Rheumatoid arthritis (RA) is a systemic autoimmune disease characterized by chronic joint inflammation and one of the main causes of chronic disability worldwide with high prevalence in the ageing population. RA is characterized by autoantibody production, synovial inflammation and bone destruction, whose most accepted biomarker is rheumatoid factor (RF) autoantibodies. In this work, we developed a low-cost approach for the detection and quantification of the RF marker. This colorimetric immunosensor is based on gold nanoprobe crosslinking that results in extensive aggregation in presence of the pentameric IgM RF. Aggregation of the nanoconjugates yields color change from red to purple that can be easily observed by the naked eye. The interaction between nanoconjugates and specific target was confirmed via dynamic light scattering (DLS), Raman spectroscopy and atomic force microscopy (AFM) imaging. This conceptual system shows a LOD of 4.15 UA/mL IgM RF (clinical threshold is set for 20 IU/mL). The one-step biosensor strategy herein proposed is much faster than conventional detection techniques, without the need for secondary antibodies, additional complex washing or signal amplification protocols. To the best of our knowledge this is the first report on target induced aggregation of gold nanoprobes for a quantitative colorimetric autoantibodies detection.

Introduction

The Rheumatoid arthritis (RA) is a complex, chronic autoimmune disorder characterized by inflammation and destruction of synovial joints.[1] Approximately 1% of the world population is affected by the disease, with the incidence among women being 2 to 3 times higher than in men.[2] Even though the complete etiology of the disease is not fully understood, interactions between genome and environment triggering abnormal immune system regulation have been suggested to be one of the probable causes of RA. Several studies have tried to identify and characterize optimal biomarkers of the disease that could be used for the early detection and diagnosis of RA but, the complex nature of the disease and patients heterogeneity in terms of symptoms and responses, hampered the clear identification of suitable diagnosis biomarkers.[3] Still, according to the American College of Rheumatology (ACR) and the European League against Rheumatism (EULAR) 2010 criteria, the rheumatoid factor (RF) and the anti-cyclic citrullinated peptide (anti-CCP) are key biomarkers for an early detection of RA.[4] More recently other diagnostic biomarkers that can help the early diagnosis/prognosis of RA have been identified such as the anti-mutated citrullinated vimentin (MCV) antibody, the anti-carbamylated proteins (CarP) antibody as well as the 14-3-3 Ƞ protein belonging to the family of 14-3-3 chaperonins, but additional guidelines for their use need to be implemented,[4] Another factor for patients' under diagnosis is the lack of laboratory facilities capable to rapidly screen the required samples.[5] The possibility to screen at point-of- care would allow to provide timely diagnostics and therapeutic intervention, thus reducing the burden on health care systems. Hence, a rapid detection system capable to specifically screen markers on a single platform might be able to enhance diagnosis and assist early therapeutic intervention, thus improving the quality of life of patients.

In recent years, gold nanoparticles (AuNPs) have been widely used as transducers in biosensing devices.[6] Among these conceptual devices, those relying on the unique optical properties of colloidal solutions of AuNPs have been used for the development of simple to use colorimetric sensor for biomolecular diagnostics.[7] The unique optical properties of colloidal gold derive from the localized surface plasmon resonance (LSPR), which can be easily tuned to provide for biodetection signal transduction.[8] The LSPR peak position is dependent on the size, shape and interparticle distance of the nanoparticles (NPs), which can be induced by changes to the media dielectric and/or by cross-linking mediated by relevant biomolecules.[9] Dispersed 15 nm diameter AuNPs show a maximum absorption at ca. 520 nm that red-shifts to ca. 600−800 nm upon aggregation. This significant change in peak absorption may be easily observed by the naked eye and quantitatively followed by UV−vis spectrophotometry.[8] The use

[a] UCIBIO, Departamento de Ciências da Vida, Faculdade de Ciências e Tecnologia, Universidade NOVA de Lisboa, Campus de Caparica, 2829-516 Caparica, Portugal; *Correspondence: pmvb@fct.unl.pt
[b] CENIMAT|i3N, Departamento de Ciência dos Materiais, Faculdade de Ciências e Tecnologia, Universidade NOVA de Lisboa, Campus de Caparica, 2829-516 Caparica, Portugal.
Electronic Supplementary Information (ESI) available: [details of any supplementary information available should be included here]. See DOI: 10.1039/x0xx00000x

View Article Online
DOI: 10.1039/C9AN00319C

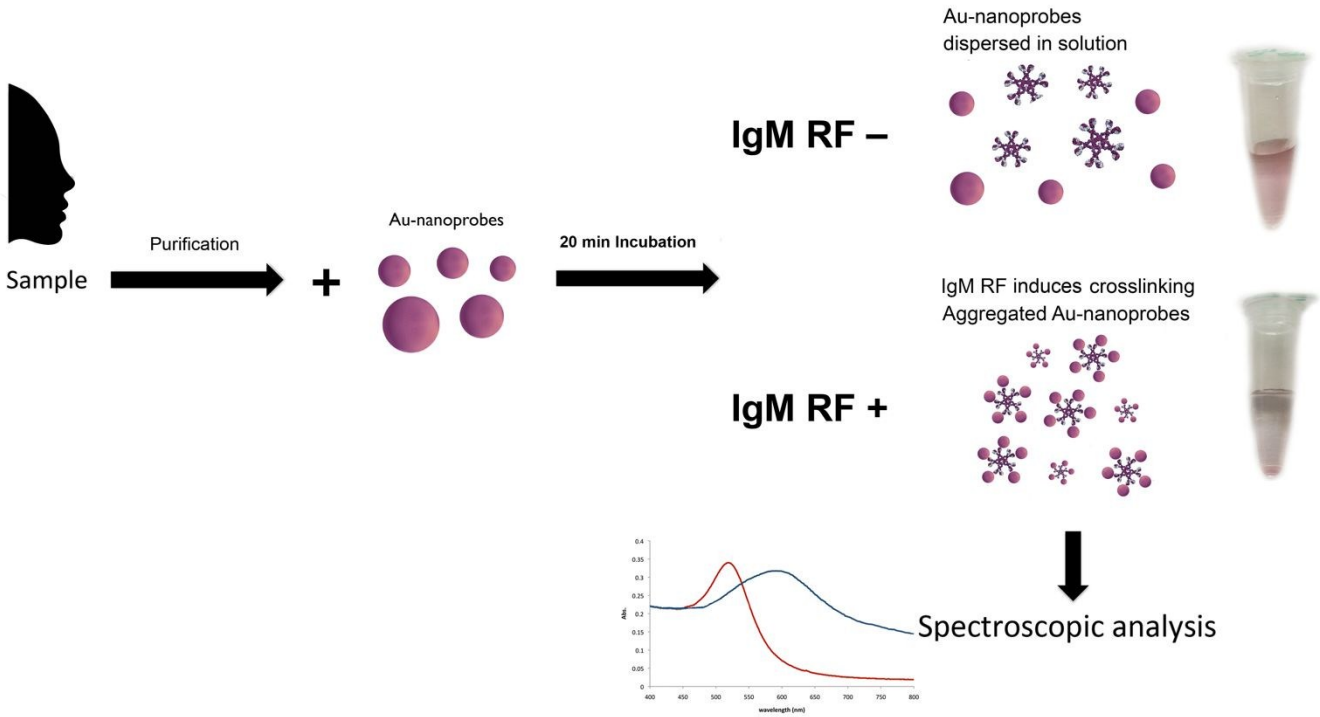

Figure 1. Au-nanoprobe for RA diagnostics. Schematic representation of the Au-nanoprobe detection of the early RA biomarker - IgM RF, whose colorimetric output provides for the readout. IgM-RF by specifically binding to the nanoconjugates, induces Au-nanoprobe aggregation, which in terms leads to a change to the LSPR peak that can be followed by UV-vis spectroscopy. On the right: actual photos of real detection samples to illustrate color discrimination by the naked eye.

of AuNPs for immunosensing shows the advantage of a one-to-one interaction between the gold nanoprobe and the specific target, allowing for an increased sensitivity and modulation of specificity with remarkable flexibility.

Here, we developed a single step colorimetric detection method to quantify RA biomarkers, specifically immunoglobulin M (IgM) RF, which bind to the Fc regions of immunoglobulin G (IgG) molecules. Although predominantly encountered as IgM, RF can be of any isotype of immunoglobulins. IgM RF detection has been the established method for routine screening since it has a multimeric structure giving it the greatest agglutinating ability.[3,4,10] In this detection scheme, the earlier biomarker of disease, IgM RF, acts as a crosslinking agent, promoting aggregation of the gold-nanoprobes, inducing a shift of the LSPR peak and concomitant color of the solution. The pentameric structure of the IgM RF factor becomes the core of a star like AuNP structure that promotes the plasmon coupling without the need of additional reagents and, thus, provides a linear response of the sensor to the concentration of biomarker.

Results and discussion

RA diagnostics is commonly performed by ELISA aiming at detecting the presence of RF in plasma samples from patients - IgM RF at a clinical threshold set for 20 IU/mL.[11] Toward the development of a one-step biosensor strategy for a simpler and faster of IgM RF without the need for additional complex wash or signal amplification protocols, we used AuNPs functionalized with IgG Fc portion. The IgG Fc will act as bait for the avid IgM RF.[4]

Gold nanoparticles with an average diameter of ~14 nm were synthesized by the citrate reduction method described by Lee and Meisel.[12] Briefly, 250 ml of 1mM $HAuCl_4$ were heated, and the solution was refluxed for 15 min. Afterwards, the solution was left at room temperature to cool down. The synthesized AuNPs were subsequently conjugated with the bi-functional polyethylene glycol (PEG) via the thiol group, leaving the carboxylic terminal available for further conjugation to reactive primary amines of the IgG Fc molecule.[13] The stabilized AuNPs-PEG-COOH were functionalized at 25% and 50% surface area coverage, and then covalently modified with human IgG Fc antibody fragment (AuNP@IgG Fc) at ratios of antibody:AuNP between 5 and 15. Functionalization efficiency and probe activity were assessed by a dot blot assay. A direct correlation between the Ab bound to the AuNP surface and probe activity was found. Moreover, a higher surface coverage with PEG-COOH allowed for increased probe activity (see supplementary information I). Also, functionalization with ratios above 15 Ab per AuNP resulted in crosslinking between nanoparticles and subsequent aggregation.

Further characterization by dynamic light scattering (DLS) and atomic Force microscopy (AFM) provides confirmation of

View Article Online
DOI: 10.1039/C9AN00319C

the interaction between the Au-nanoprobe and the IgM RF (Figure 2). Au-nanoprobes with IgM RF positive and negative controls in a molar ratio of 5 Ab:Au-nanoprobe were incubated for 60 minutes and diluted to a final concentration of 0.25 nM. For the AFM analysis, samples were dropped onto mica sheets and allowed to dry in a vacuum chamber (Figure 2). Data show that, in the presence of the IgM RF, the Au-nanoprobes gathered in a structure around the pentameric IgM target, thus forming a distinctive pentamer where the IgM RF is decorated by 5 individual gold nanoparticles. However, without the IgM RF, i.e. the specific target for the avid IgG Fc at the surface of the AuNPs, no such structure is observed. (Figure 2B). The presence of ordinary IgMs (not RF) in human plasma did not induce the formation of these pentameric structures as shown by DLS and AFM data (Figure 2B right).

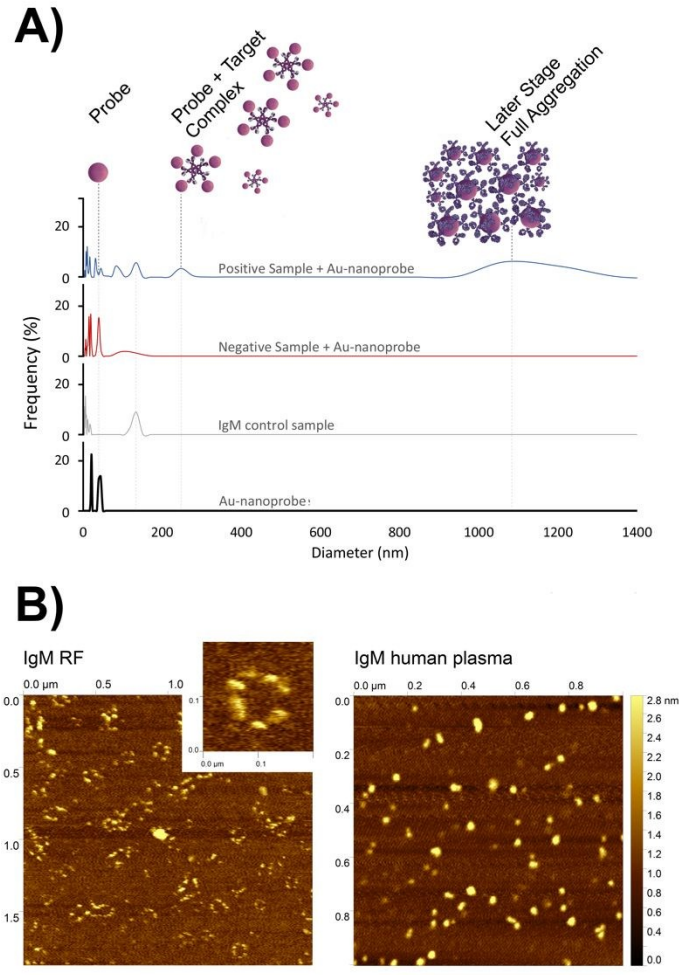

Figure 2. Au-nanoprobe: target complex characterization. **A)** DLS analysis of 50% PEG-COOH@15 IgG Fc Au-nanoprobe; target sample (IgM and IgM RF) and Probe+ target complex. Concentration of 500 IU/mL of IgM RF was incubated for a period of 60 minutes before measurement. Frequency (%) in number. **B)** AFM characterization of Au-nanoprobe: target complex; topograph of Au-nanoprobe with IgM RF complex (left), topograph of Au-nanoprobe with IgM from human plasma (right).

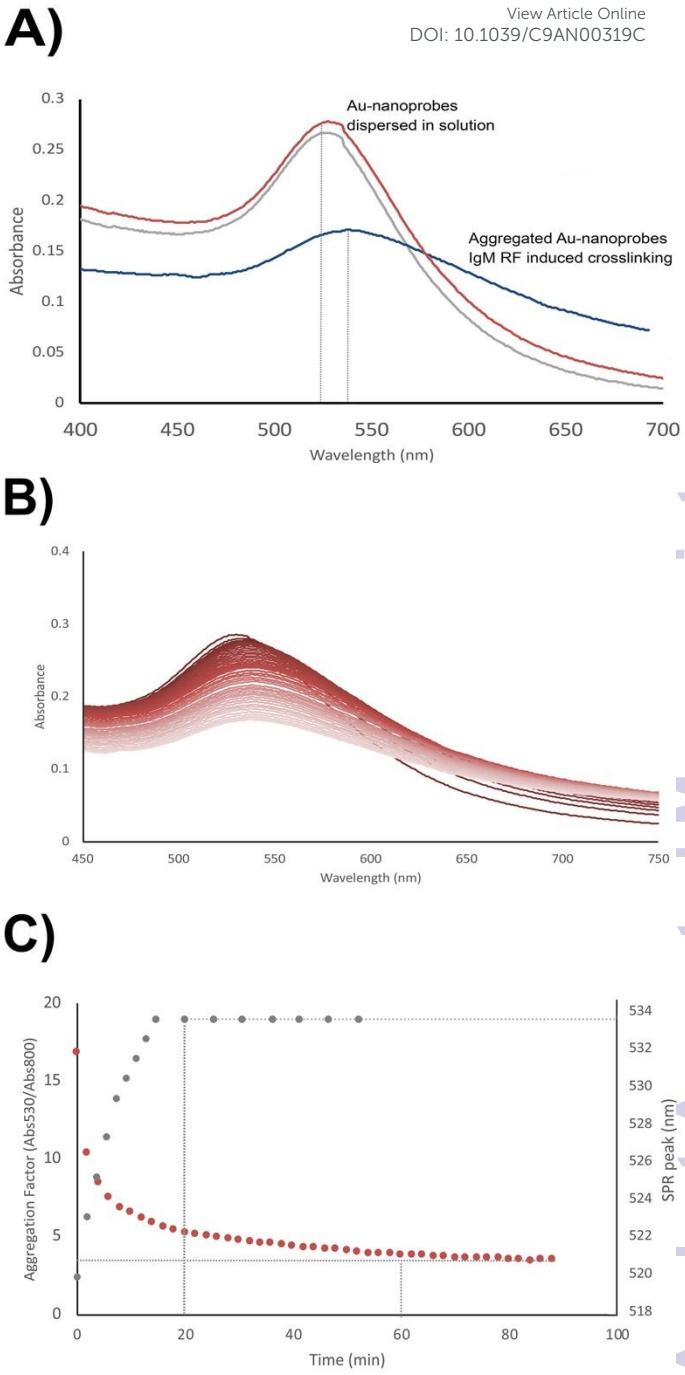

Figure 3. Au-nanoprobe colorimetric detection. **A)** Absorbance spectra for Au-nanoprobes (50% PEG-COOH@15-IgG-Fc): (●) Au-nanoprobes (50% PEG-COOH 15-IgG-Fc) after addition of IgM RF and (●) IgM from human plasma solutions. (●) Au-nanoprobe spectra without addition of any target sample. Concentration of 500 IU/mL of IgM-RF. **B)** Absorbance spectra for Au-nanoprobes PEG-COOH@IgG-Fc) taken every 2 minutes after addition of IgM RF. **C)** Aggregation kinetic analysis followed by the ratio of Abs(530nm/580nm) (Red) and max SPR wavelength (Grey).

View Article Online
DOI: 10.1039/C9AN00719G

Following the characterization of probe activity and probe: target specific interaction, AuNP@IgG Fc nanoprobes were used for the development of the IgM RF colorimetric detection assay. Increasing amounts of IgM RF in solution were added to the synthesized Au-nanoprobes. An IgM antibody solution extracted from human plasma was used as negative control. In the presence of the specific target - IgM RF, a color change from pink to purple was observed; whereas there was no change to the solution's color in the case of IgM from human plasma or buffer controls (Figure 3A). UV–vis spectroscopy analysis shows that, following IgM RF addition to the Au-nanoprobe solution, a decrease of the characteristic AuNP@IgG FC LSPR peak at ca. 520 nm is observed, coupled to a distinguishable red-to ca. 538 nm (Figure 3).

We further characterized the kinetics of this target specific induced aggregation (Figure 3). The aggregation process starts with the complexation of the Au-nanoprobes and the IgM RF target, followed by the red-shift to the nanoprobe´s LSPR from ca. 520 nm to ca. 538 nm. This process steadies after 20 minutes, after which no further change to the maximum LSPR value is detected. However, a decrease in the absorbance at 538nm is noticed. This decrease is often associated with the development of large aggregates that subsequently precipitate at the bottom of the reaction tube, leading to fewer aggregates in solution and a concomitant decrease to the perceived intensity (Figure 1 – aggregated nanoprobe IgM RF crosslinking photograph). This precipitation process stabilizes after 70 minutes of incubation time (Figure 3).

The interaction between the target IgM RF and the specific Au-nanoprobe was further confirmed by Raman spectroscopy. It is well known that Raman signals are dramatically enhanced on the surface of metallic nanostructures - surface-enhanced Raman scattering (SERS), which has been widely used for biodetection schemes.[14] This same principle can also be used to detect and characterize molecular interactions between a nanostructured probe and target.[14] Raman spectral analysis was performed to highlight and further corroborate the specific interaction between IgM RF and the Au-nanoprobes (Figure 4).

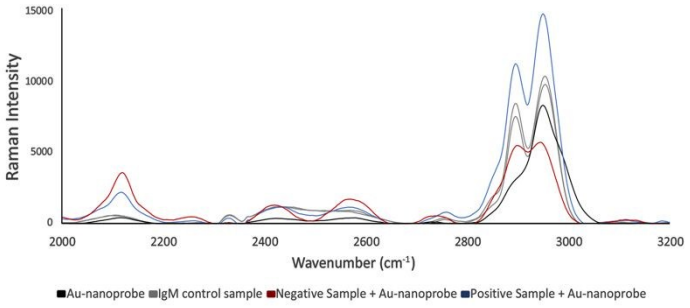

Figure 4 Raman spectra of the Au-nanoprobe: target complex. **A)** Raman spectra of (AuNPs@IgGhFC) Probe; target sample (IgM and IgM RF) and Probe+ target complex. Concentration of 500 IU/mL of IgM RF was incubated for a period of 60 minutes before measurement.

Despite the detection of several characteristic peaks, an overlap between those related to the Au-nanoprobe and target was observed. These vibrational modes correspond mainly to the polypeptide sequence present in both the probe and target samples. The IgM signal is divided into characteristic peaks at 2890 cm^{-1} and 2990 cm^{-1}. The results show that the intensity of the Raman signal of the target sample is enhanced when the Au-nanoprobe:IgM RF complex is present. The increased intensity of IgM RF peaks in the presence of Au-nanoprobe demonstrates the enhancement effect at the gold nanoparticles´ surface when the target is in close vicinity. Interestingly, the intensity of the Raman signal attributed to the IgM from human serum shows a decay in presence of the Au-nanoprobes. This clearly demonstrates that a specific interaction between Au-nanoprobe and target is needed for Raman signal amplification. Moreover, the Au-nanoprobe may add an internal filter like effect that decreases the Raman signal for the non-specific antibodies that are not directly interacting with the probe´s surface. Additionally, microscope images of the samples show a clear difference in the macroscopic distribution of Au-nanoprobes between IgM RF positive and negative samples. Presence of IgM RF induces a clear aggregation/flocculation with a change in color of the scattered light (see Supplementary Information Figure S2). These results corroborate the specific interaction of the IgM RF with the Au-nanoprobe and show the feasibility of this low volume and highly sensitive approach for the detection of IgM RF.

To determine the detection limit of the colorimetric approach, the Au-nanoprobe solution was incubated with increasing amounts of IgM in TBS buffer (molar ratio of IgM:Au-nanoprobe ranging from 0; 0.1; 0.2; 0.4; 0.5; 0.6;1;2;5. After 30 minutes of incubation, UV–vis spectra were recorded, and Absorbance changes were monitored via the shift to the maximum LSPR value. A direct correlation between the molar ratio of IgM RF sample and red-shift of the LSPR was observed (Figure 5).

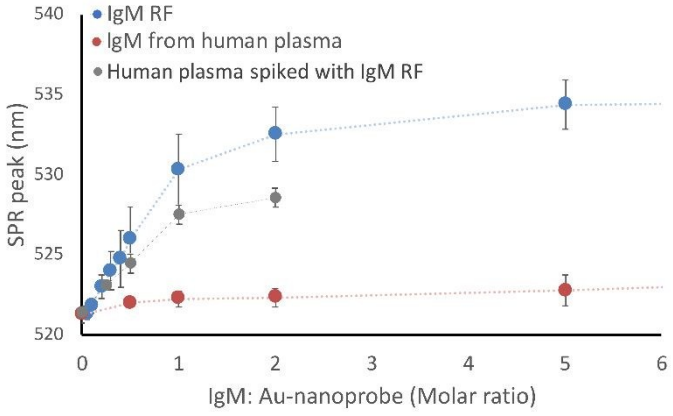

Figure 5. Au-nanoprobe colorimetric detection. Calibration curves for the Au-nanoprobe with increasing amounts of IgM RF and control samples. (●) IgM RF (●) IgM from human plasma; (●) Human plasma spiked with igM RF. Results are expressed as function of the IgM to Au-nanoprobe molar ratio. Error bars represent SD with a minimum of three independent experiments.

View Article Online
DOI: 10.1039/C9AN00319G

This shift in the LSPR was not present in the case of the IgM sample from human plasma. This correlation is significant for ratios above 0.2 IgM RF/Au-nanoprobe (1.6 IU/mL) and increases further until a maximum at a ratio of 5 (41.5 IU/mL). The lowest measured IgM RF concentration that gives the statistically significant difference from that of the negative was 0.5 IgM RF/Au-nanoprobe (4.15 IU/mL); therefore, this should be considered the actual LOD. Additionally, human plasma samples were spiked in with IgM RF. Data show that for lower concentrations of IgM RF, the LSPR shift was similar to that of the IgM RF calibration curve. A lesser shift of the peak was observed for the human plasma matrix (ratio of IgM RF/Au-nanoprobe > 0.5). Still, the LOD for the method remains unaltered. The linear correlation between LSPR peak shift and concentration of specific target in solution, may provide for a direct/single step (semi-)quantitative IgM RF detection.

The flexibility of the detection scheme herein presented may provide for valuable advantages for the management of rheumatoid arthritis by providing a valuable tool for diagnostics. In fact, several scenarios may be conceived: i) higher concentrations of Au-nanoprobe may be used for direct visual colorimetric detection, i.e. without specialized instruments (since the standard threshold for positive/negative is 20 IU/mL, the nanoprobe concentration may be increased four times for visual screening without compromising performance); ii) the system permits a reduction in Au-nanoprobe concentration, improving detection of IgM RF in extremely low concentrations - 4.15 IU/mL; iii) the system may provide for a semi-quantitative determination of the autoantibody since there is a direct correlation between signal and IgM RF concentration.

Experimental

All reagents were purchased from Sigma Aldrich and were of analytical grade. IgM RF Antibodies from human plasma (Ref. 180603) were purchased from Hözel Diagnostika Handels GmbH (Köln, Germany), IgM from human serum (Ref.I8260) was purchased from Sigma-Aldrich (Missouri, U.S.A.). Human IgG fragment crystallizable region (Fc region) was purchased from ThermoFisher Scientific (Massachusetts, U.S.A).

AuNP synthesis and conjugation to human IgG-Fc

Gold nanoparticles were prepared by the citrate reduction method described by Lee and Meisel.[23] Briefly, 250 ml of 1 mM $HAuCl_4$ was brought to a boil while stirring in a 500 ml round-bottom flask. Twenty-five milliliters of 38.8 mM sodium citrate were quickly added, and the mixture refluxed for 15 min with continuous stirring. The flask was left to cool down to room temperature and stored in the dark until use. The average size of the NPs was obtained by analysis of TEM images. Conjugation of human IgG-Fc to the AuNPs was performed as previously described[15] using a bi-functional polyethylene glycol (PEG) [COOH–PEG-SH (458.57g.mol^{-1}) (Iris Biotech GmbH)] linker with a thiol group for direct bonding to the gold surface and a carboxylic group for conjugation to reactive primary amines in the Fc portion of the human IgG. The AuNP solution (15 nM) was incubated with 0.013 mg of the bi-functional PEG, the excess reagents removed by centrifugation at 13 800g for 30 minutes and the red precipitate redispersed in milli-Q water. Then, 10 nM of these AuNP@PEG were allowed to react with 5 mmol of N-(3-dimethylaminopropyl)-N'-ethylcarbodiimide hydrochloride (EDC) and 7.5 mmol of N-hydroxysulfosuccinimide sodium salt (sulfo-NHS) in 10 mM 2-(N-morpholino) ethanesulfonic acid (MES) buffer (pH 6.5) for 30 minutes at 37 °C. The AuNPs were washed by centrifugation to remove the excess of EDC and sulfo-NHS. The AuNPs were then incubated with a human IgG-Fc antibody for 2 hours at 37 °C in 10 mM MES buffer (pH 6.5). The uncoupled antibody (Ab) was washed by centrifugation and the AuNP conjugates resuspended in 10 mM sodium phosphate buffer (pH 8) for 30 minutes. The Ab-AuNP nanoconjugates were stored at 4 °C in 50 mM Tris-buffered saline (TBS) buffer (pH 8).[15]

Dynamic Light Scattering (DLS) analysis

The colloidal stability and the hydrodynamic diameter of the nanoconjugates were assessed by DLS with a Horiba SZ-100 NanoPARTICA Analyzer. Each sample was subjected to 2000 measurements with 3 runs each. For the IgM RF Au-nanoprobe complex characterization, the nanoconjugates were incubated with 5 IgM RF in a 1:5 ratio for one hour before analysis.

Dot Blot assay

The efficiency of the coupling protocol was assessed by a standard dot blot assay using an DEMEDITEC Diagnostics GmbH Rheumatoid Factor IgM-RF ELISA determination kit (Kiel-Wellsee, Germany). The synthetized Au-nanoprobe was deposited (2.5 nM) on nitrocellulose membrane Protran BA79 0.1 µm (Whatman). Then, 3 droplets were deposited per spot in a volume of 6 µL per spot, and the membranes allowed to dry at room temperature. Following Au-nanoprobe deposition onto the nitro-cellulose membrane and blocking with 5% (w/v) milk solution in 50mM Tris-buffered saline with 0.1% (v/v) Tween 20 (TBST), blots were incubated per manufacturer's instructions for 1 hour at room temperature with primary antibodies IgM RF (500 IU/mL). Membranes were washed with TBST buffer and incubated with the appropriate secondary antibody (Ab) conjugated with horseradish peroxidase (reference no. 7074 or 7076, Cell Signaling Technology). Advansta WesternBright ECL (C.A., U.S.A.) was applied to the membranes, and signal acquired in a Gel Doc imager (Bio-Rad, U.S.A). The image files were analyzed with LI-COR Imagestudio software to determine the relative intensity of each spot. All data are expressed as mean ± standard deviation from at least three independent experiments.

Atomic Force Microscopy (AFM)

IgM RF Au-nanoprobe complex topology was evaluated following 1:100 dilution of the original solution on a freshly cleaved mica sheet and allowed to dry for two hours in a vacuum chamber. All AFM measurements were done in an Asylum Research MFP-3D Standalone system operated in alternate contact mode in air and under ambient conditions, with a minimum resolution of 256 x 1024 pixels. Two types of commercially available silicon probes were used throughout

View Article Online DOI: 10.1039/C9AN00719C

this study: Olympus AC160TS (f_0=300 kHz; k=26 N/m) by Olympus Corporation (Tokyo, Japan) and SSS-NCHR (f_0=330 kHz; k=42 N/m) by Nanosensors (Neuchâtel, Switzerland). In order to enhance contrast between objects of interest and the background, the produced topographs were flattened and had their scale range limited to exclude outlier values of over at most 3 times the RMS value of the image.

Raman spectroscopy

Raman measurements were carried out with a Renishaw® inVia™ Qontor® confocal Raman microscope equipped with a Renishaw Centrus 2957T3 detector and a laser operating at 50 mW and at 633 nm. The spectra were recorded as an extended scan. The laser beam was focused with a 50× Olympus objective lens (N10.6 LMPLAN FL N). All of the measurements were made with an integration time of five scans and 25 seconds of exposure time. The intensity of the incident laser was reduced to 175 µW (10%) on the surface of the sample by suitable filtering to prevent sample degradation. A 2 µl drop of each test sample under the same conditions and same preparation procedure previously used for AFM analysis were used. The spectrograph was calibrated using the Raman line at 521 cm^{-1} of a Si wafer for reducing possible fluctuations of the Raman system. All SERS spectra were recorded at room temperature, and no observable spectrograph fluctuations of the Raman system were observed. Spectra data expressed as mean from three independent experiments.

IgM-RF detection assay

IgM-RF detection protocol assay was performed by incubating the Au-nanoprobes at a concentration of 2.5nM with increasing molar ration amounts of IgM RF and IgM from human plasma (molar ratio used: 0, 0.2; 0.4; 0.5; 0.6; 1; 2; 5) in TBS buffer in a final volume of 30 µL. Following 20 minutes incubation at room temperature visible spectra were acquired in a Shimatzu UVmini-1240 spectrophotometer (Kyoto, Japan). Intensity and shifts of LSPR peaks measured and data expressed as mean ± standard deviation from at least three independent experiments.

All the IgM RF antibodies used in this work were assessed with the DEMEDITEC Diagnostics GmbH Rheumatoid Factor IgM-RF ELISA determination kit (Kiel-Wellsee, Germany) to allow correlation between concentration and activity.

Conclusions

The Au-nanoprobe assay herein reported allows for a quantitative analysis of RF with a LOD of 4.15 IU/mL (above the standard threshold of 20 IU/mL). The linear relationship between the analytical signal and target concentration was demonstrated to be related to the probe concentration allowing for a flexible tuning of the detection approach. Also, it may be used in several types of samples (e.g. serum, synovial fluid and urine), taken that the appropriate antibody purification process is used.

This detection approach is much faster than classic determination methods, such as ELISA immunoassays, and there is no need for additional signal amplification. This makes it promising for quick, reliable, and cost-effective screening of rheumatoid arthritis. Results can be obtained in a short time in a one-step procedure, without the need for multistep procedures used in traditional immunoassay approaches. Moreover, we demonstrate the use of Au-nanoprobes to specifically enhance the Raman scattering of the target IgM RF allowing for an extremely low volume and highly sensitive approach for non-contact and non-destructive sample analysis that could be easily integrated into a microfluidic chip like approach. This sensing approach makes the RA molecular screening and subsequent diagnosis much easier, both by lowering the costs as well as by providing a robust assay instead of labour-intensive techniques, thus allowing for application at decentralized locations and even at point-of-care.

Conflicts of interest

There are no conflicts to declare.

Acknowledgements

This work was supported by the Unidade de Ciências Biomoleculares Aplicadas-UCIBIO which is financed by national funds from FCT/MEC (UID/Multi/04378/2013) and co-financed by the ERDF under the PT2020 Partnership Agreement (POCI-01-0145-FEDER-007728). This work was partially supported by the European Commission under project INNO INDIGO 2015 – RA Detect: One Platform- Multiple biomarker detection of Rheumatoid Arthritis (https://radetect.eu/). B. Veigas was supported by FCT/MEC (SFRH/BPD/124311/2016).

References

1 Q. Guo, Y. Wang, D. Xu, J. Nossent, N.J. Pavlos and J. Xu, *Bone Res.*, 2018, **6**, 15; D. L. Scott, F. Wolfe and T. W. J. Huizinga, *Lancet*, 2010, **376**, 1094.

2 S. Thakur, B. Riyaz, A. Patil, A. Kaur, B. Kapoor and V. Mishra, *Biomed. Pharmacother*., 2018, **106**, 1011.

3 D. S. Gibson, M. E. Rooney, S. Finnegan, J. Qiu, D. C. Thompson, J. Labaer, S. R. Pennington and M. W. Duncan, *Rheumatology* (Oxford), 2012, **51**(3), 423; M. A. van Leeuwen, J. Westra, P. L. van Riel, P. C. Limburg and M. H. van Rijswijk, *Scand. J. Immunol*., 1995, **24**(3), 146; D. A. Carson, P. P. Chen, R. I. Fox, T. J. Kipps, F. Jirik, R. D. Goldfien, G. Silverman, V. Radoux and S. Fong, *Annu. Rev. Immunol.,* 1987, **5**, 109.

4 A. Swart, R. W. Burlingame, I. Gürtler and M. Mahler, *Clin. Chim. Acta.*, 2012, **414**, 266; J. Ursum, W. H. Bos, N. van Dillen, B. A. Dijkmans and D. van Schaardenburg, *Arthritis. Res. Ther.*, 2010, **12**(1), R8; R. Aggarwal, K. Liao, R. Nair, S. Ringold and K. H. Costenbader, *Arthritis. Rheum.*, 2009, **61**(11), 1472; B. I. Gavrilă, C. Ciofu and V. Stoica, *J. Med. Life.*, 2016, **9**(2), 144.

5 P. W. Meyer, M. M. Ally and R. Anderson, *Rheumatol. Int.*, 2016, **36**(6), 751; P. E. Chandra, J. Sokolove, B. G. Hipp, T. M. Lindstrom, J. T. Elder, J. D. Reveille, H. Eberl, U. Klause and W. H. Robinson, *Arthritis. Res. Ther.*, 2011, **13**(3), R102.

Analyst ARTICLE

View Article Online
DOI: 10.1039/C9AN00319C

6 G. Doria, J. Conde, B. Veigas, L. Giestas, C. Almeida, M. Assunção, J. Rosa, P. V. Baptista, *Sensors* (Basel), 2012, **12**(2), 1657.

7 P. V. Baptista, G. Doria and J. Conde, *Proc. SPIE*., 2011, 7909; R. Chandrawati, M.M. Stevens, *Chem Commun (Camb)*, 2014, **50**(41), 5431; A. Kaur, O. Shimoni, M. Wallach, *World J Gastroenterol,* 2018, **24**(47), 5379; A.J. Caires, H.S. Mansur, A.A.P. Mansur, S.M. Carvalho, Z.I.P. Lobato, J.K.P. Dos Reis. *Colloids Surf B Biointerfaces*. 2019, 177:377; Y.H. Cheng, Y.F. Cheung, T. Siu-Chung Tam, C.N. Lok, H. Sun, K.M. Ng. *Anal Chim Acta*. 2019, 1055, 1.

8 J. Wilcoxon, *J. Phys. Chem. B*., 2009, **113**(9), 2647.

9 L. Soares, A. Csáki, J. Jatschka, W. Fritzsche, O. Flores, R. Franco and E. Pereira, *Analyst*, 2014, **139**(19), 4964; F. Tian, F. Bonnier, A. Casey, A. E. Shanahan and H. J. Byrne, *Analytical Methods*, 2014, **6**, 9116; B. Sajjanar, B. Kakodia, D. Bisht, S. Saxena, A. K. Singh, V. Joshi, A. K. Tiwari and S. Kumar, *J. Nanopart. Res.*, 2015, **17**, 234; A. Lesniewski, M. Los, M. Jonsson-Niedziółka, A. Krajewska, K. Szot, J. M. Los and J. Niedziolka-Jonsson, *Bioconjug. Chem.,* 2014, **25**(4), 644.

10 A. L. Corper, M. K. Sohi, V. R: Bonagura, M. Steinitz, R. Jefferis, A. Feinstein, D. Beale, M. J. Taussig and B. J. Sutton, *Nat. Struct. Biol.*, 1997, **4**(5), 374.

11 L. Gossec, M. Dougados, P. Goupille, A. Cantagrel, J. Sibilia, O. Meyer, J. Sany, J. P. Daurès and B. Combe, *Ann. Rheum. Dis.*, 2004, **63**(6), 675; A. Saraux, J. M. Berthelot, G. Chalès, C. Le Henaff, J. Y. Mary, J. B. Thorel, S. Hoang, M. Dueymes, J. Allain, V. Devauchelle, D. Baron, P. Le Goff and P. Youinou P, *Arthritis Rheum.,* 2002, **47**(2), 155.

12 P. C. Lee, D. Meisel, *J. Phys. Chem.*, 1982, **86**, 3391.

13 S. Puertas, P. Batalla, M. Moros, E. Polo, P. Del Pino, J. M. Guisan, V. Grazú, J. M. de la Fuente, *ACS Nano*, 2011, **5**(6), 4521; E. Polo, P. del Pino, B. Pelaz, V. Grazu, J. M. de la Fuente, *Chem. Commun.* (Camb), 2013, **49**(35), 3676; J. T. Dias, L. Lama, J. Gantelius and H. Andersson-Svahn, *Nanoscale*, 2016, **8**(15), 8195.

14 Y. Zhang, S. Zhao, J. Zheng and L. He, *Trends in Analytical Chemistry*, 2017, **90**, 1; M. Vendrell, K. K. Maiti, K. Dhaliwal and Y. T. Chang, *Trends Biotechnol.*, 2013, **31**(4), 249; J. Baniukevic, I. Hakki Boyaci, A. Goktug Bozkurt, U. Tamer, A. Ramanavicius and A. Ramanaviciene, *Biosens. Bioelectron.*, 2013, **43**, 281; S. McAughtrie, K. Faulds and D. Graham, *Journal of Photochemistry and Photobiology C: Photochemistry Reviews*, 2014, **21**, 40; R. P. Kengne-Momo, Ph. Daniel, F. Lagarde, Y. L. Jeyachandran, J. F. Pilard, M. J. Durand-Thouand and G. Thouand, *Journal of Spectroscopy*, 2012, **462901**, 1.

15 J. Conde, A. Ambrosone, V. Sanz, Y. Hernandez, V. Marchesano, F. Tian, H. Child, C. C. Berry, M. R. Ibarra, P. V. Baptista, C. Tortiglione and J. M. de la Fuente, *ACS Nano*, 2012, **6**(9), 8316; M. J. Fischer, *Methods. Mol. Biol.*, 2010, **627**, 55; N. A. Byzova, I. V. Safenkova, E. S. Slutskaya, A. V. Zherdev and B. B. Dzantiev, *Bioconjug. Chem.*, 2017, **28**(11), 2737.

View Article Online
DOI: 10.1039/C9AN00319C

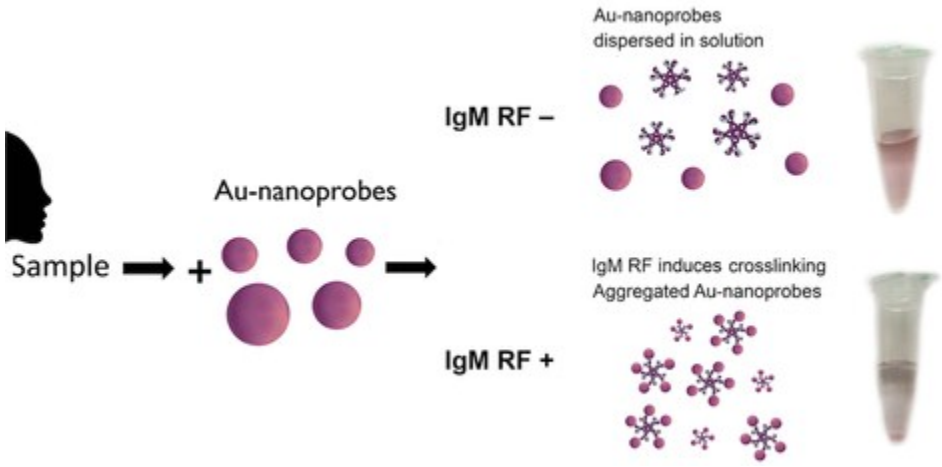

39x19mm (300 x 300 DPI)